Nano Energy (▮▮▮▮) ▮, ▮▮▮–▮▮▮

Available online at www.sciencedirect.com

SciVerse ScienceDirect

journal homepage: www.elsevier.com/locate/nanoenergy

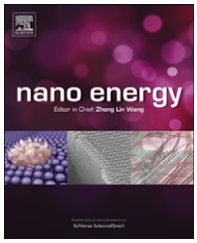

RAPID COMMUNICATION

The effect of metallic coatings and crystallinity on the volume expansion of silicon during electrochemical lithiation/delithiation

Matthew T. McDowell[a], Seok Woo Lee[a], Chongmin Wang[b], Yi Cui[a,c,*]

[a]*Department of Materials Science and Engineering, Stanford University, Stanford, CA 94305, USA*
[b]*Environmental Molecular Sciences Laboratory, Pacific Northwest National Laboratory, Richland, WA 99354, USA*
[c]*Stanford Institute for Materials and Energy Sciences, SLAC National Accelerator Laboratory, 2575 Sand Hill Road, Menlo Park, CA 94025, USA*

Received 23 February 2012; received in revised form 8 March 2012; accepted 8 March 2012

KEYWORDS
Energy storage;
Batteries;
Silicon anode;
Nanowire;
In-situ transmission electron microscopy

Abstract
Applying surface coatings to alloying anodes for Li-ion batteries can improve rate capability and cycle life, but it is unclear how this second phase affects mechanical deformation during electrochemical reaction. Here, in-situ transmission electron microscopy is employed to investigate the electrochemical lithiation and delithiation of silicon nanowires (NWs) with copper coatings. When copper is coated on only one sidewall, the NW bilayer structure bends during delithiation due to length changes in the silicon. Tensile hoop stress causes conformal copper coatings to fracture during lithiation without undergoing bending deformation. In addition, in-situ and ex-situ observations indicate that a copper coating plays a role in suppressing volume expansion during lithiation. Finally, the deformation characteristics and dimensional changes of amorphous, polycrystalline, and single-crystalline silicon are compared and related to observed electrochemical behavior. This study reveals important aspects of the deformation process of silicon anodes, and the results suggest that metallic coatings can be used to improve rate behavior and to manage or direct volume expansion in optimized silicon anode frameworks.

Introduction

Materials that alloy with lithium at low potentials, such as silicon, germanium, and tin, have among the highest volumetric and gravimetric capacities of known negative electrode materials and show great promise for replacing commercial

*Corresponding author at: Department of Materials Science and Engineering, Stanford University, Stanford, CA 94305, USA. Tel.: +650 723 4613; fax: +650 725 4034.
E-mail address: yicui@stanford.edu (Y. Cui).

2211-2855/$ - see front matter © 2012 Elsevier Ltd. All rights reserved.
http://dx.doi.org/10.1016/j.nanoen.2012.03.004

graphite in next-generation Li-ion batteries [1,2]. Silicon in particular has been studied extensively due to its relative abundance, low toxicity, and high gravimetric capacity (about ten times that of graphite) [3]. One of the main challenges preventing the implementation of silicon-based negative electrodes is the ~300% volume change that occurs during lithiation/delithiation of silicon particles [3,4]. These large volume changes can cause mechanical fracture and loss of electrical contact with the current collector, which results in capacity fade. In recent years, silicon nanostructures, including nanowires (NWs) [5], nanotubes [6–8], hollow particles [9], and nanoparticles [10,11] have shown improved cycling performance over conventional micron-size electrode particles. The smaller size of these nanostructured particles results in a lower propensity for fracture [12–14].

Although silicon nanostructures have shown promising performance, the details regarding volume changes during reaction have only recently begun to be understood; this knowledge is important for designing structures with optimum shape and size for reversible lithiation/delithiation. In-situ atomic force microscopy experiments on silicon thin films have shown that the films increase and decrease in height reversibly during lithiation and delithiation [15]. More recently, our group and others reported that crystalline silicon expands anisotropically upon first lithiation, with {110} surfaces swelling preferentially [16–18]; this could theoretically cause unforeseen stress states to exist. Along these lines, we have shown that this anisotropic expansion strongly influences fracture of silicon nanopillars: cracks form at the surface between adjacent {110} planes during lithiation, which indicates that these regions experience intensified tensile hoop stress due to anisotropic expansion [19]. In addition, in-situ transmission electron microscopy (TEM) studies on silicon NWs by Liu et al. have shown that similar cracks can develop along the NW axis during lithiation [17]. Ghassemi et al. have used in-situ TEM to study volume expansion and phase changes in amorphous silicon [20], and other in-situ TEM results have shown that carbon coating on silicon NWs increases the lithiation rate and helps to ensure full lithiation of the material [4]. We have also studied the constraining effect of oxide layers on silicon nanostructures, and finite element modeling showed that an oxide layer can induce significant hydrostatic compressive stresses in very small silicon nanostructures, which could alter the equilibrium concentration of lithium in silicon [13]. Finally, a number of models have been developed to study the mechanics of the lithiation/delithiation process [21–25].

Overall, these studies have indicated that crystalline orientation and surface coatings influence volume expansion, but there are still open questions in this area. For instance, the morphological and volume changes in amorphous and polycrystalline nanostructures during reaction with lithium need to be compared to commonly-investigated single-crystalline nanostructures. In addition, a number of reports have shown that coating silicon with an inactive metal, especially copper, results in better rate performance, higher Coulombic efficiency, and better capacity retention with cycling [26–29]. The electrical conductivity of copper, 5.96×10^5 S cm^{-1}, is much higher than that of lithiated silicon (~1–10 S cm^{-1} [30]), so copper is an ideal coating for improving electrical conductivity. More importantly, however, the copper coating apparently results in a more stable electrolyte interface with fewer side reactions, and it has been postulated that a copper coating acts as a "glue" that binds silicon particles together to prevent electronic isolation during expansion and contraction [26]. Although copper coatings have resulted in promising performance, the effects of an inactive metallic coating on silicon volume changes have not been experimentally documented. In a recent study, Yang et al. modeled the stresses and bending curvature in copper–silicon bilayer structures during lithiation and delithiation [31]. In an in-situ TEM study be Zhang et al., it was shown that aluminum, copper, and carbon coatings could suppress radial expansion in SnO_2 NWs [32], but it is not clear what effect such coatings have on the expansion of silicon nanostructures. In this paper, we report in-situ and ex-situ TEM and scanning electron microscopy (SEM) results regarding the interrelated effects of copper coating and silicon crystallinity on the structural, morphological, and volumetric changes of silicon NWs during lithiation/delithiation.

Materials and methods

In-situ TEM experiments

The in-situ experiments were carried out using a dual probe Nanofactory STM-TEM holder that allows for the fabrication and testing of a nanoscale electrochemical cell in a similar manner as recent reports [33]. Figure 1a shows a low-magnification TEM image and schematic of the experimental setup. Silicon NWs were first grown on silicon substrates using the vapor–liquid–solid (VLS) method with 50 nm gold nanoparticles as the catalyst [34], and copper was deposited on some samples with either thermal evaporation or sputtering (AJA International ATC Orion, 5 mTorr pressure, 150 W of power, and 15 sccm argon flow). Thermal evaporation is highly directional, and it results in a copper layer on a single sidewall of the NWs. Sputtering causes copper to uniformly coat the entire surface of many of the NWs since the process is intrinsically less directional and the substrate was also rotated within the sputtering chamber during deposition. A few NWs were removed from the substrate and attached to one of the gold metal probes of the TEM holder, as shown in Figure 1a. $LiCoO_2$ powder was attached to the other gold probe with conductive epoxy, and a drop of ionic liquid electrolyte was placed on this electrode. The ionic liquid electrolyte consisted of 10 wt% lithium bis(trifluoromethylsulfonyl) imide (LiTFSI) in a solvent of 1-butyl-1-methylpyrrolidinium bis(trifluoromethylsulfonyl) imide (P_{14}TFSI). Inside the microscope (FEI Titan), the NW electrode was positioned so that the tips of a few NWs were submerged in the liquid electrolyte while most of their length remained out of the electrolyte in the field of view. A bias of −4 V was applied with respect to the $LiCoO_2$ electrode, which caused lithium ions to be reduced at the NW electrode and to diffuse into the NWs from the electrolyte as the NWs became lithiated. For delithiation, the voltage was removed and the two probes were effectively shorted together, which causes the NWs to become delithiated as the lithium diffused back into the ionic liquid electrolyte.

Please cite this article as: M.T. McDowell, et al., The effect of metallic coatings and crystallinity on the volume expansion of silicon during electrochemical lithiation/delithiation, Nano Energy (2012), http://dx.doi.org/10.1016/j.nanoen.2012.03.004

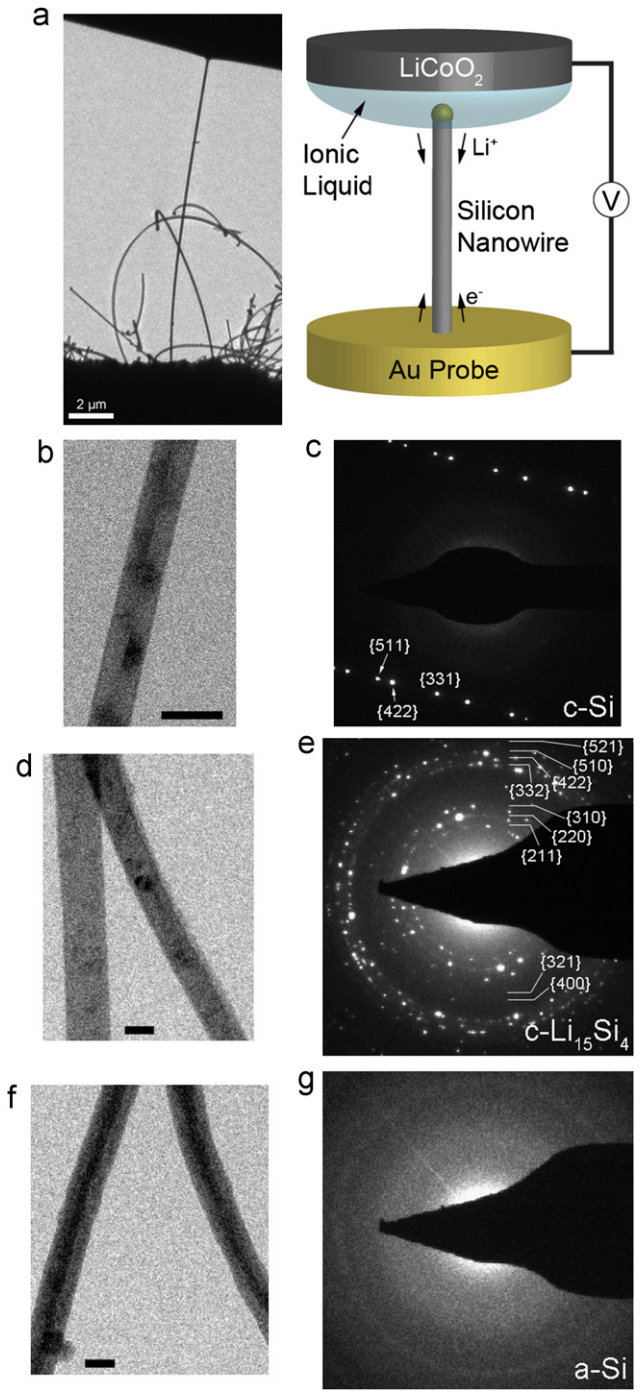

Figure 1 (a) In-situ electrochemical cell built on a TEM-STM holder. The TEM image on the left shows a silicon NW spanning the gap between the conductive gold probe (bottom) and the ionic liquid-coated $LiCoO_2$ counter electrode (top). The tip of the NW is inserted into the liquid at the top of the image where a meniscus is visible. The accompanying schematic on the right shows the geometry of the cell. (b, c) TEM image and SAED pattern of a pristine single-crystalline NW with a twin defect. (d, e) TEM image and SAED pattern of fully lithiated NWs. The NWs are polycrystalline with the cubic $Li_{15}Si_4$ crystal structure. (f, g) TEM image and SAED pattern of delithiated NWs. After delithiation, the NWs contract in diameter, and the SAED pattern suggests that they have transformed into amorphous silicon. All unlabeled scale bars are 100 nm.

Ex-situ TEM experiments

Ex-situ experiments were also performed on single-crystalline, polycrystalline, and amorphous NWs. Single crystalline silicon NWs were first grown directly on 304 stainless steel substrates from 50 nm gold nanoparticles. To fabricate polycrystalline and amorphous NWs, as-grown NWs on steel substrates were inserted into pouch-type electrochemical half cells with lithium metal as the counter/reference electrode, and the NWs were lithiated by sweeping at 0.1 mV/s to 40 mV vs. Li/Li^+ and holding for 10 h, and then they were delithiated by sweeping to 2 V and holding for 10 h. After delithiation, the NW electrodes were removed and cleaned with acetonitrile and hydrochloric acid to etch away the solid electrolyte interphase (SEI). At this point, the NWs were amorphous. To make polycrystalline NWs, these amorphous NWs were annealed at 750 °C under flowing argon for 2 h. For ex-situ TEM tests, single-crystalline, polycrystalline, and amorphous NWs on which copper was evaporated were lithiated in pouch cells by holding at 50 mV vs. Li/Li^+ for 10 h using an Arbin battery tester. The electrodes were removed in an Ar-filled glove box (MBraun USA), washed with acetonitrile, and transferred to carbon film TEM grids for TEM analysis in an FEI Tecnai TEM.

Nanopillar fabrication

Silicon nanopillars (NPs) for ex-situ SEM tests were fabricated as described in a previous study [16]. Briefly, 600 nm diameter silica spheres were first fabricated through a modified Stober synthesis and were then drop-cast on a ⟨110⟩ silicon wafer for use as an etch mask. Reactive-ion etching using the Bosch process with modified process conditions was employed to create pillars ~3–4 μm in length, and then the silica etch mask was removed with HF etching. The ⟨100⟩ wafer on which the pillars stood could then be used directly in pouch-type electrochemical cells as the working electrode. The SEM used for ex-situ observation was an FEI Sirion XL30.

Results and discussion

In-situ TEM experiments

Figure 1(b–g) shows in-situ TEM images detailing the lithiation and delithiation process for initially single-crystalline silicon NWs without copper coating. Figure 1(b and c) shows a TEM image (b) and selected area diffraction (SAED) pattern (c) of a NW with a twin that runs along the axis; this type of defect is relatively common in VLS-grown silicon NWs. Figure 1(d) shows similar NWs after full lithiation in-situ. During the early stages of lithiation, the NWs transform into an amorphous Li–Si alloy, which subsequently crystallizes into polycrystalline $Li_{15}Si_4$, as shown in Figure 1(e) and reported previously [4,35]. During delithiation, the lithium diffuses out of the NWs back into the electrolyte, and the NWs shrink radially and revert to amorphous silicon. Figure 1(f) shows an image of fully delithiated NWs, and Figure 1(g) is the associated SAED pattern. From Figure 1(f), the center of the NWs appears darker, signifying greater thickness or density in this region; this indicates that the

Please cite this article as: M.T. McDowell, et al., The effect of metallic coatings and crystallinity on the volume expansion of silicon during electrochemical lithiation/delithiation, Nano Energy (2012), http://dx.doi.org/10.1016/j.nanoen.2012.03.004

distribution of silicon in the delithiated NWs is inhomogeneous and skewed toward the center. These in-situ results are similar to those previously reported by Liu et al., although in that study intrinsic single-crystalline NWs were reported to be incompletely lithiated [4], whereas here intrinsic NWs are observed to form the completely lithiated $Li_{15}Si_4$ phase.

In comparison to Figure 1, Figure 2(a) shows a single-crystalline NW that has ~20 nm of copper evaporated onto the left sidewall, as illustrated in the accompanying schematic. The NW does not bend after copper deposition. After lithiation (Figure 2b), the NW transforms into the polycrystalline $Li_{15}Si_4$ phase and remains straight; the copper layer does not deform significantly during volume expansion. This is because during lithiation, the NW expands primarily in the radial direction due to anisotropic expansion [16,17]. The vast majority of the NWs tested had ⟨211⟩ axial orientations, which means there are two {110} sidewalls that expand preferentially while there is negligible axial expansion. If the NW were to expand along the axial direction during lithiation, one would expect bending of the composite structure and perhaps fracture of the copper layer due to tensile stress. Since radial expansion dominates, this allows the evaporated layer to remain intact, which is beneficial for maintaining high electrical conductivity along the NW. Upon delithiation, the silicon NW/copper composite structure immediately starts to bend with the copper layer on the outside of the bent structure, as shown in Figure 2(c). This indicates that there is both axial and radial shrinkage; the NW contracts in a more isotropic manner than it expands, as has been reported for bare NWs [4]. The consistently observed result after delithiation is a NW that is bent or buckled along its whole length due to the dimensional mismatch between the copper and silicon, as shown in the low magnification image in Figure 2(d). The copper layer remains intact and does not fracture because it experiences compressive stress, which is again beneficial for maintaining high electrical conductivity in the composite structure.

Figure 3(a) shows a TEM image of a single-crystalline silicon NW coated uniformly with a ~20 nm thick copper layer by sputtering. This case is different than before since the copper layer completely encapsulates the NW, as shown in the schematic and magnified image in Figure 3(a). After full lithiation to the $Li_{15}Si_4$ phase (Figure 3b), the NW remains straight, but the copper layer fractures parallel to the axis due to tensile hoop stress that develops during radial expansion of the NW. This is in contrast to the in-situ observations made by Zhang et al. on uniformly carbon-coated SnO_2 NWs; these NWs expanded primarily along the axis during lithiation and caused the coating layer to fracture perpendicular to the axial direction because of axial tensile stress in the coating [32]. In addition, thin metal and carbon coatings on SnO_2 NWs in this previous study were observed to completely suppress radial expansion and favor axial expansion, whereas in the present study on silicon NWs, even thicker (~50 nm) conformal copper coatings fracture and do not suppress radial expansion to the same degree as that observed in SnO_2 NWs (see Supplementary Figure S1). As shown in Figure 3(c), delithiation does not cause

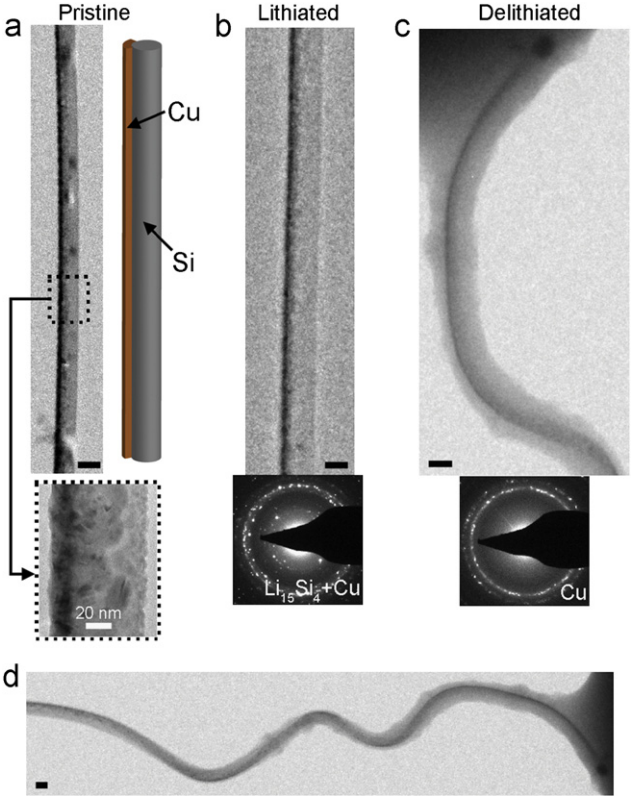

Figure 2 In-situ lithiation/delithiation process for a silicon NW with a ~20 nm copper layer evaporated onto one side. (a) TEM images and schematic of a pristine single-crystalline NW with copper (darker contrast) on the left sidewall. (b) TEM image and SAED pattern of a similar fully lithiated NW. (c) TEM image and SAED pattern of a delithiated NW. The top of the NW is immersed in ionic liquid electrolyte. The NW is bent with the copper layer on the outer edge because the silicon undergoes axial contraction during delithiation. (d) A low-magnification view of the same delithiated NW showing bending along the entire length. All unlabeled scale bars in this figure are 100 nm.

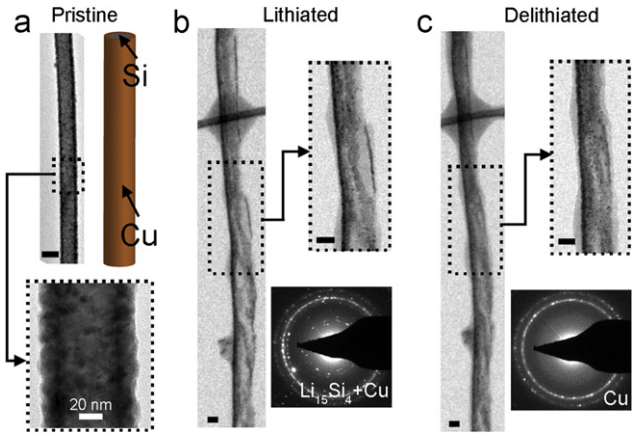

Figure 3 In-situ lithiation/delithiation process for a silicon NW with a ~20 nm thick conformal copper coating. (a) TEM images and schematic of a pristine single-crystalline NW coated with copper. The copper coating surrounds the entire NW. (b) TEM images and SAED pattern of a similar lithiated NW. The copper layer has fractured due to the influence of tensile hoop stress. (c) TEM images and SAED pattern of the same NW after delithiation. Diameter contraction causes the cracks in the copper to partially heal, but there is no bending of the composite structure. All unlabeled scale bars are 100 nm.

Please cite this article as: M.T. McDowell, et al., The effect of metallic coatings and crystallinity on the volume expansion of silicon during electrochemical lithiation/delithiation, Nano Energy (2012), http://dx.doi.org/10.1016/j.nanoen.2012.03.004

bending in the composite structure because the copper constraint is present on all sides of the NW instead of just on one side as in the previous case. Instead, the NW remains straight after delithiation, and contraction along the radial direction causes the cracks in the copper layer to shrink and become partially "healed," as shown in the magnified images of the same NW in Figure 3(b and c). NWs coated with both deposition methods become amorphous after delithiation, and the crystal structure of the copper is not affected during the lithiation/delithiation process since it is inert to lithium reaction.

To gain deeper insight into the physical processes occurring during lithiation, Figure 4 presents two series of images captured from videos taken during the in-situ lithiation of NWs that have been coated by evaporation (one side coated, Figure 4a) and sputtering (all sides coated, Figure 4c). The videos are available in the supplementary information. Figure 4(a (i)) shows a pristine 85 nm-diameter silicon NW that has ~20 nm of copper evaporated on the left sidewall. The NW is inserted into the ionic liquid above the image frame, and this image was recorded right before this portion of the NW began to react with lithium. After nine seconds (Figure 4a (ii)), the upper portion of the wire has begun to expand as the Li-Si reaction front, marked by the arrow on the right side of the NW, moves into the frame. After 17 s (Figure 4a (iii)), the reaction front has advanced toward the bottom of the frame. After 36 s (Figure 4a (iv)), the initial reaction front has passed, but the NW is still expanding radially as the crystalline core continues to be lithiated. After 393 s of lithiation, the diameter of the NW has expanded to ~150 nm. Figure 4(b) shows a series of schematics that correspond to the images in Figure 4(a); these schematics illustrate the initial expansion of the NW as the reaction front passes and then the continued gradual outward expansion as the crystalline core becomes fully lithiated. An interesting feature of this lithiation process is

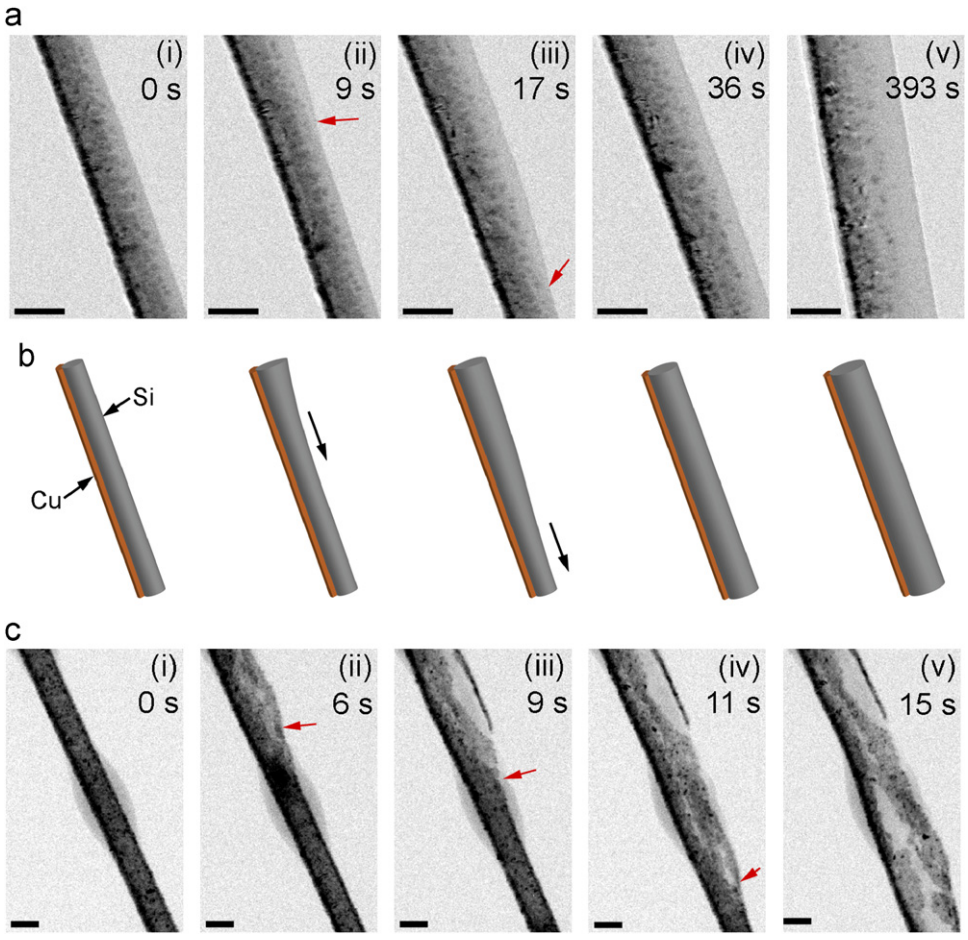

Figure 4 Image series showing the lithiation process in NWs with different copper coatings. The lithium source is out of the frame above the images. (a) Lithiation of a NW with copper deposited on one side. The arrows in frames (ii) and (iii) denote the edge of the reaction front as it proceeds down the NW. Expansion primarily occurs away from the copper layer, and the copper does not fracture. (b) Series of schematics corresponding to the image frames in (a) illustrating the initial expansion away from the copper layer as the reaction front proceeds down the NW. The black arrows in the second and third frames denote the direction of movement of the reaction front that consumes crystalline silicon near the surface of the NW. After the reaction front has passed, the remaining crystalline silicon core of the NW becomes gradually lithiated, as illustrated by the more uniform radial expansion in the later schematics. (c) Lithiation of a NW with a conformal copper coating. Again, the arrows mark the position of the reaction front. The copper fractures as the NW expands, and these cracks affect the direction of subsequent expansion. A thin drop of ionic liquid that flowed down from the reservoir is visible in the middle of the NW throughout the lithiation process. All scale bars are 100 nm.

Please cite this article as: M.T. McDowell, et al., The effect of metallic coatings and crystallinity on the volume expansion of silicon during electrochemical lithiation/delithiation, Nano Energy (2012), http://dx.doi.org/10.1016/j.nanoen.2012.03.004

that during the initial advance of the reaction front, the NW is observed to expand primarily on the opposite side of the copper coating. The reaction front is visible in panels (ii) and (iii) as a bump on the right side of the NW, but there is no corresponding bump on the side with copper coating. This behavior was observed consistently for samples of this type.

In Figure 4(a), the reaction front was observed to proceed along the axis of the NW at a velocity of 50 nm s^{-1}. The average axial reaction front velocity for all of the copper-coated NWs tested in this study was 69 nm s^{-1}, which is an order of magnitude higher than that previously reported for uncoated NWs [4]. During lithiation, lithium reacts near the surface first as the reaction front moves axially down the NW, but a crystalline silicon core remains after the reaction front passes. After the passing of the primary reaction front, lithiation continues as radial lithium diffusion causes the remaining crystalline silicon core to be converted into amorphous Li–Si and then crystalline $Li_{15}Si_4$.

Similar observations can be made for the copper sputter-coated NW in Figure 4(c). A section of unreacted wire is shown in Figure 4(c (i)); the NW is initially ~75 nm in diameter, and the copper layer is 15–20 nm thick. Six seconds later (Figure 4c (ii)), the reaction front has moved down into the image frame. After nine seconds (Figure 4c (iii)), the reaction front has proceeded further and the top of the NW has expanded significantly, resulting in fracture of the copper coating. At 11 s (Figure 4c (iv)), the reaction front is near the bottom of the image frame and the copper on the lower section of the NW has begun to fracture. Finally, after 15 s, the reaction front has completely passed, causing additional fracture to occur in the copper coating due to the influence of tensile hoop stress. The expansion of this NW causes two primary cracks to form: one extending into the top of the frame and the other into the bottom. As the copper fractures, it seems that the underlying silicon has greater freedom to expand through the newly formed crack. After fracture at the top of the NW, the silicon expands primarily to the right towards the crack opening, but at the bottom of the frame, the NW expands more evenly. This is further evidence that copper plays a role in directing volume expansion.

Ex-situ experiments

In-situ experiments such as these are extremely valuable for studying the dynamic processes of lithiation and delithiation, but there is an important difference between the in-situ experimental arrangement and that of a real battery: in a battery, the NWs are completely immersed in electrolyte. As such, ex-situ experiments are also important, although they cannot provide the same detailed information as in-situ experiments. Here, we employ ex-situ scanning electron microscopy (SEM) observations to investigate further the role of a copper layer in suppressing volume expansion. For these experiments, silicon nanopillars (NPs) are used instead of silicon NWs. These NPs are fabricated from ⟨110⟩ silicon wafers by reactive ion etching (RIE) and have well-defined crystallographic orientations. The wafer with NPs on the surface is used directly as the working electrode in an electrochemical cell, and the NPs can be lithiated, removed from the cell, and transferred to the SEM chamber for viewing.

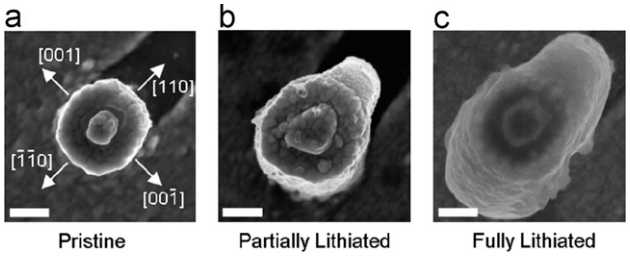

Figure 5 Ex-situ SEM images of silicon nanopillars directionally coated with copper before and after lithiation. (a) Top-down image of a pristine ⟨110⟩ axially-oriented silicon nanopillar with crystallographic directions labeled. A 100 nm thick copper coating has been deposited on the lower left ($\bar{1}\bar{1}$0) sidewall. (b) Similar nanopillar after partial lithiation by holding at 120 mV vs. Li/Li^+ for 10 h. The uncoated (110) sidewall at the upper right has expanded, while the coated ($\bar{1}\bar{1}$0) sidewall has not. (c) A nanopillar after deep lithiation by holding at 10 mV for 10 h. The uncoated (110) sidewall has expanded to a greater degree, and the ($\bar{1}\bar{1}$0) sidewall has also slightly expanded. It is clear that the copper coating acts to suppress expansion at the ($\bar{1}\bar{1}$0) sidewall. All scale bars are 200 nm.

Figure 5(a) is a top-down SEM image that shows the cross section of a single ⟨110⟩ axially-oriented pristine pillar before lithiation. This pillar is ~400 nm in diameter and has a height of a few microns, and a 100 nm thick copper coating has been evaporated onto the lower left ($\bar{1}\bar{1}$0) sidewall. Previous work has shown that holding such pillars at intermediate lithiation voltages (120 mV vs. Li/Li^+) causes the surface region to expand and amorphize while the core remains crystalline silicon [16]. For uncoated pillars of this axial orientation, expansion would occur preferentially at the two {110} sidewalls. In contrast, for pillars coated with copper as in Figure 5, partial lithiation at 120 mV results in volume expansion primarily on the uncoated (110) sidewall, as seen in Figure 5(b). This confirms our in-situ observations and indicates that even in a fully-flooded electrochemical cell geometry, the copper coating can suppress lithiation. After deep lithiation of the nanopillars by holding at 10 mV (Figure 5c), the nanopillar expands further on the uncoated side, but less significant expansion is also evident on the ($\bar{1}\bar{1}$0) sidewall that has the copper coating. Overall, copper probably acts as both a mechanical constraint and a barrier to lithium ion diffusion in suppressing the expansion of silicon. Nanostructured copper has been reported to be able to sustain much larger stresses and strains than the bulk form [36], so these films could exert substantial stresses on the Li–Si alloy as it expands. In addition, previous work has found that a 100 nm thick planar coating of copper slowed the reaction kinetics of silicon thin films when reacting with lithium [26], which indicates that the copper coatings on the NWs and NPs could slow lithium diffusion and result in the lesser degree of volume expansion observed in our experiments.

In addition to studying the interaction of copper and silicon during lithiation-induced deformation, copper coating can also give insight into the intrinsic deformation mechanisms of silicon nanostructures of different crystalline character. To explore this avenue, we have fabricated amorphous, polycrystalline, and single-crystalline silicon NWs with a copper layer evaporated on a single sidewall (see Methods for details). Through

Please cite this article as: M.T. McDowell, et al., The effect of metallic coatings and crystallinity on the volume expansion of silicon during electrochemical lithiation/delithiation, Nano Energy (2012), http://dx.doi.org/10.1016/j.nanoen.2012.03.004

ex-situ TEM observation before and after lithiation of these structures in conventional electrochemical cells, the deformation behavior can be correlated to crystal structure. Figure 6(a–c) show example TEM images of pristine single-crystalline (a), polycrystalline (b), and amorphous (c) NWs and associated SAED patterns. The pristine NWs of each type are generally straight. Figure 6(d) displays galvanostatic electrochemical signatures for the first charge/discharge cycle of electrodes made from each type of NW without copper coating in conventional half cells. The single-crystalline NWs (solid line) show a relatively flat two-phase plateau at ~125 mV upon lithiation (discharge) that corresponds to the conversion of the crystalline silicon to amorphous Li–Si [37]. The polycrystalline NWs show a similar two-phase plateau, but it is at a lower potential and displays a slight nucleation barrier; these features were consistently observed. This could be due to a decrease in reaction kinetics and/or a lower equilibrium lithiation voltage due to the random orientation of crystalline grains within the NW. A random granular orientation would mean that the crystalline surfaces that are exposed to the electrolyte at the NW sidewalls are not necessarily the preferentially lithiated {110} surfaces as in the single-crystalline NWs, which would shift the reaction potential since first-principles modeling has shown that the different surfaces exhibit different electrochemical potentials [38]. The amorphous NWs initially react at a higher potential via a single-phase mechanism, but after about 65% of the total capacity is reached, the three curves follow approximately the same path, indicating similar electrochemical behavior and physical transformations. Upon delithiation (charge), the three curves are also similar.

Ex-situ TEM observation after lithiation reveals that many of the individual NWs undergo bending deformation since the silicon changes dimensions due to lithium insertion while the copper only passively deforms. Figure 6(e–g) show typical TEM images of single-crystalline (e), polycrystalline (f), and amorphous (g) NWs after lithiation by holding at 50 mV vs. Li/Li^+ and subsequent transfer to a carbon-coated TEM grid. From the SAED pattern in Figure 6(h), all of these NWs are amorphous after this treatment, indicating that there is probably some delithiation of the reactive Li–Si NWs during the washing and transfer process. However, we think the NWs are only partially delithiated since they still show evidence of volume expansion, as detailed below. This example of a change in chemical state of the NWs is one of the limitations of the ex-situ experimental process, but in this case valuable information can still be obtained from these experiments.

From the typical TEM images in Figure 6(e–g), the curvature of the NW/copper bilayer structure after lithiation is different for each type of NW. The curvature of the bilayer is related to the axial dimensional change in the silicon: if the bilayer bends with the copper layer on the outside of the structure, the silicon NW has decreased in length, while the opposite is true when the copper layer

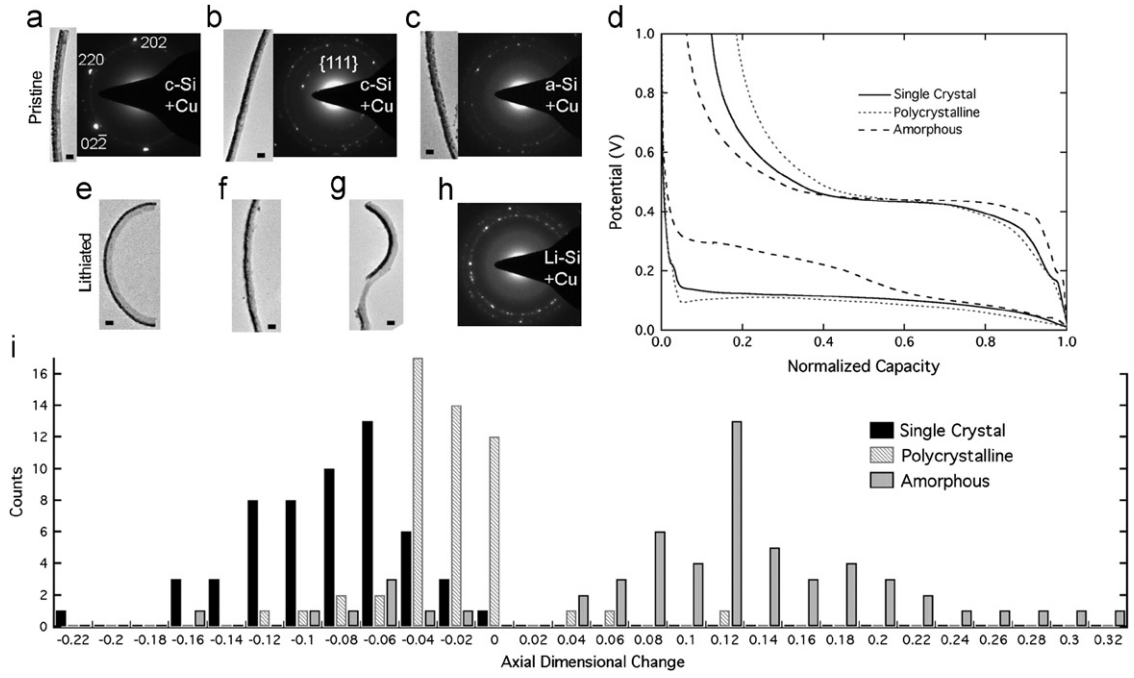

Figure 6 Ex-situ TEM and electrochemical behavior of single-crystalline, polycrystalline, and amorphous silicon NWs. (a–c) TEM images and SAED patterns of pristine single-crystalline (a), polycrystalline (b), and amorphous (c) NWs with copper deposited on the left sidewalls. (d) First cycle galvanostatic curves for each type of NW without copper coating in conventional pouch-type cells. (e–g) Typical ex-situ images of single-crystalline (e), polycrystalline (f), and amorphous (g) NW/copper bilayers after lithiation in pouch cells by holding at 50 mV vs. Li/Li^+. The three types of NWs with different initial crystalline character show different bending behavior. (h) Typical SAED pattern showing that the NWs are amorphous after lithiation during ex-situ imaging. (i) Bar chart showing the calculated axial dimensional change for many single-crystalline, polycrystalline, and amorphous NWs. The axial dimensional change is calculated from the radius of curvature measured from the ex-situ TEM images of the bent NWs. The three types of NWs show dissimilar bending behavior: single-crystalline and polycrystalline NWs show different degrees of length contraction, while amorphous NWs show length extension upon lithiation and ex-situ imaging. All scale bars in this figure are 100 nm.

Please cite this article as: M.T. McDowell, et al., The effect of metallic coatings and crystallinity on the volume expansion of silicon during electrochemical lithiation/delithiation, Nano Energy (2012), http://dx.doi.org/10.1016/j.nanoen.2012.03.004

is on the inner surface of the bent structure. Figure 6(i) presents statistical data showing the axial dimensional change for many lithiated NWs of each type. The axial dimensional change $\Delta L/L$ is calculated from the measured radius of curvature by employing the geometrical expression $\Delta L/L=(1/2)\kappa\ t$, where ΔL is the length change, L is the initial length, κ is the curvature, and t is the thickness of the silicon–copper bilayer structure. This expression is derived from simply considering the curvature necessary to match the lengths of adjacent surfaces of two bent beams of different lengths, and as such, it does not incorporate any mechanical effects such as plastic deformation in the Cu layer. However, it does allow for an estimate of the length change of different NWs for comparative purposes. From Figure 6(i), the single-crystalline NWs decrease in length after the electrochemical treatment, with $\Delta L/L$ values ranging from -0.22 to -0.02 with an average of -0.09. From the in-situ observations, similar single-crystalline NWs were observed to maintain the same length after lithiation; this again suggests that the NWs are partially delithiated when observed ex-situ. The polycrystalline NWs also primarily show axial shrinkage, but to a lesser degree than the single-crystalline NWs (average $\Delta L/L=-0.03$). Finally, the amorphous Si NWs generally increase in length, with an average $\Delta L/L$ value of 0.10. These differences in axial dimensional change can be directly related to the different lithiation processes that occur in the different types of NWs. The two-phase reaction that occurs as crystalline silicon is converted to amorphous Li–Si happens preferentially at {110} surface facets, which are on the sidewalls of the $\langle 211 \rangle$ axially oriented single-crystalline NWs. This results in negligible length change during lithiation and the observed length contraction due to slight delithiation before ex-situ imaging. For the polycrystalline NWs, the preferentially lithiated {110} facets are oriented more randomly at each grain along the NW, which results in a greater observed value of axial dimensional change in Figure 6(i). Finally, the amorphous NWs undergo a single-phase lithiation process that results in more isotropic expansion, as evidenced by the increase in length in Figure 6(i). Overall, this data demonstrates that the structure of a silicon anode must be carefully designed to account for the different expansion behavior for silicon with different crystallinity. An initially crystalline structure will undergo dissimilar volume expansion after the first cycle when it is amorphous, and this must be considered when applying coatings or physically arranging the structures in an electrode framework.

Conclusion

In summary, we have utilized in-situ and ex-situ electron microscopy to study the effect of copper coating and silicon crystallinity on volume expansion and morphological changes during lithiation and delithiation. Copper coating on a single sidewall allows for volume expansion without fracture of the copper layer, while uniform copper coatings fracture during the lithiation of the NW. The copper coating was also observed to partially suppress silicon expansion during lithiation in in-situ and ex-situ experiments. Copper coatings have been shown to increase Coulombic efficiency and improve rate capability, and this study shows that the choice of silicon crystallinity and the location of the copper coating affect volume expansion and morphological changes. This suggests that copper coatings can be used to direct the expansion of silicon; such engineering is important to create optimized electrode frameworks to manage volume expansion and contraction.

One of the major remaining obstacles preventing the use of silicon in Li-ion batteries is that silicon-based anodes typically exhibit lower Coulombic efficiency than graphite anodes. High Coulombic efficiency is extremely important for long cycle life of a full battery cell. The formation of the solid electrolyte interphase (SEI) contributes to lower Coulombic efficiency, and the new surfaces that are repeatedly exposed to the electrolyte during the large volume changes in silicon-based anodes could promote excessive SEI formation. Since copper coatings have been shown to improve Coulombic efficiency (although not to the level of graphite anodes), it seems that the copper-electrolyte interface promotes more stable SEI formation than does bare silicon. If this is the case, it is desirable to create a copper coating that does not fracture during charge or discharge, exposing the inner silicon to the electrolyte. From the data here, conformal copper coatings fracture upon lithiation, which unfortunately would reveal the bare silicon to the electrolyte. To solve this issue, it would be useful to engineer silicon nanostructures that allow the coating layer to remain mechanically stable during silicon volume changes. An example might be a structure in which there is free space between the coating layer and the silicon that would permit unimpeded expansion while preventing electrolyte exposure.

Acknowledgments

Portions of this work are supported by the U.S. Department of Energy, Office of Basic Energy Sciences, Division of Materials Sciences and Engineering under Contract no. DE-AC02-76SF00515 through the SLAC National Accelerator Laboratory LDRD project and the Assistant Secretary for Energy efficiency and Renewable Energy, Office of Vehicle Technologies of the U.S. Department of Energy under Contract no. DE-AC02-05CH11231, Subcontract no. 6951379 under the Batteries for Advanced Transportation Technologies (BATT) Program. Y.C. acknowledges support from the King Abdullah University of Science and Technology (KAUST) Investigator Award (no. KUS-l1-001-12). M.T.M. acknowledges support from the Chevron Stanford Graduate Fellowship, the National Defense Science and Engineering Graduate Fellowship, and the National Science Foundation Graduate Fellowship. S.W.L. acknowledges support from KAUST (no. KUK-F1-038-02). C.M.W. acknowledges support from the Laboratory Directed Research and Development (LDRD) program of Pacific Northwest National Laboratory. The in-situ TEM work was conducted in the William R. Wiley Environmental Molecular Sciences Laboratory (EMSL), a national scientific user facility sponsored by DOE's Office of Biological and Environmental Research and located at PNNL. PNNL is operated by Battelle for the DOE under Contract DE-AC05-76RLO1830.

Appendix A. Supporting information

Supplementary data associated with this article can be found in the online version at http://dx.doi.org/10.1016/j.nanoen.2012.03.004.

References

[1] M.S. Whittingham, MRS Bulletin 33 (2008) 411–419.
[2] R. Marom, S.F. Amalraj, N. Leifer, D. Jacob, D. Aurbach, Journal of Materials Chemistry 21 (2011) 9938–9954.
[3] U. Kasavajjula, C.S. Wang, A.J. Appleby, Journal of Power Sources 163 (2007) 1003–1039.
[4] X.H. Liu, L.Q. Zhang, L. Zhong, Y. Liu, H. Zheng, J.W. Wang, J.-H. Cho, S.A. Dayeh, S.T. Picraux, J.P. Sullivan, S.X. Mao, Z.Z. Ye, J.Y. Huang, Nano Letters 11 (2011) 2251–2258.
[5] C.K. Chan, H.L. Peng, G. Liu, K. McIlwrath, X.F. Zhang, R.A. Huggins, Y. Cui, Nature Nanotechnology 3 (2008) 31–35.
[6] B. Hertzberg, A. Alexeev, G. Yushin, Journal of the American Chemical Society 132 (2010) 8548.
[7] M.H. Park, M.G. Kim, J. Joo, K. Kim, J. Kim, S. Ahn, Y. Cui, J. Cho, Nano Letters 9 (2009) 3844–3847.
[8] T. Song, J.L. Xia, J.H. Lee, D.H. Lee, M.S. Kwon, J.M. Choi, J. Wu, S.K. Doo, H. Chang, W. Il Park, D.S. Zang, H. Kim, Y.G. Huang, K.C. Hwang, J.A. Rogers, U. Paik, Nano Letters 10 (2010) 1710–1716.
[9] Y. Yao, M.T. McDowell, I. Ryu, H. Wu, N.A. Liu, L.B. Hu, W.D. Nix, Y. Cui, Nano Letters 11 (2011) 2949–2954.
[10] I. Kovalenko, B. Zdyrko, A. Magasinski, B. Hertzberg, Z. Milicev, R. Burtovyy, I. Luzinov, G. Yushin, Science 334 (2011) 75–79.
[11] A. Magasinski, P. Dixon, B. Hertzberg, A. Kvit, J. Ayala, G. Yushin, Nature Materials 9 (2010) 353–358.
[12] I. Ryu, J.W. Choi, Y. Cui, W.D. Nix, Journal of the Mechanics and Physics of Solids 59 (2011) 1717–1730.
[13] M.T. McDowell, S.W. Lee, I. Ryu, H. Wu, W.D. Nix, J.W. Choi, Y. Cui, Nano Letters 11 (2011) 4018–4025.
[14] C.M. DeLuca, K. Maute, M.L. Dunn, Journal of Power Sources 196 (2011) 9672–9681.
[15] L.Y. Beaulieu, T.D. Hatchard, A. Bonakdarpour, M.D. Fleischauer, J.R. Dahn, Journal of the Electrochemical Society 150 (2003) A1457–A1464.
[16] S.W. Lee, M.T. McDowell, J.W. Choi, Y. Cui, Nano Letters 11 (2011) 3034–3039.
[17] X.H. Liu, H. Zheng, L. Zhong, S. Huan, K. Karki, L.Q. Zhang, Y. Liu, A. Kushima, W.T. Liang, J.W. Wang, J.H. Cho, E. Epstein, S.A. Dayeh, S.T. Picraux, T. Zhu, J. Li, J.P. Sullivan, J. Cumings, C.S. Wang, S.X. Mao, Z.Z. Ye, S.L. Zhang, J.Y. Huang, Nano Letters 11 (2011) 3312–3318.
[18] J.L. Goldman, B.R. Long, A.A. Gewirth, R.G. Nuzzo, Advanced Functional Materials 21 (2011) 2412–2422.
[19] S.W. Lee, M.T. McDowell, L.A. Berla, W.D. Nix, Y. Cui, Proceedings of the National Academy of Sciences 109 (2012) 4080–4085.
[20] H. Ghassemi, M. Au, N. Chen, P.A. Heiden, R.S. Yassar, ACS Nano 5 (2011) 7805–7811.
[21] M.W. Verbrugge, Y.T. Cheng, Journal of the Electrochemical Society 156 (2009) A927–A937.
[22] R. Deshpande, Y.T. Cheng, M.W. Verbrugge, Journal of Power Sources 195 (2010) 5081–5088.
[23] T.K. Bhandakkar, H.J. Gao, International Journal of Solids and Structures 47 (2010) 1424–1434.
[24] K.J. Zhao, W.L. Wang, J. Gregoire, M. Pharr, Z.G. Suo, J.J. Vlassak, E. Kaxiras, Nano Letters 11 (2011) 2962–2967.
[25] K.J. Zhao, M. Pharr, Q. Wan, W.L. Wang, E. Kaxiras, J.J. Vlassak, Z.G. Suo, Journal of the Electrochemical Society 159 (2012) A238–A243.
[26] V.A. Sethuraman, K. Kowolik, V. Srinivasan, Journal of Power Sources 196 (2011) 393–398.
[27] H.X. Chen, Y. Xiao, L. Wang, Y. Yang, Journal of Power Sources 196 (2011) 6657–6662.
[28] K.F. Chiu, K.M. Lin, H.C. Lin, C.H. Hsu, C.C. Chen, D.T. Shieh, Journal of the Electrochemical Society 155 (2008) A623–A627.
[29] J.W. Kim, J.H. Ryu, K.T. Lee, S.M. Oh, Journal of Power Sources 147 (2005) 227–233.
[30] M.T. McDowell, Y. Cui, Advanced Energy Materials 1 (2011) 894–900.
[31] B. Yang, Y.P. He, J. Irsa, C.A. Lundgren, J.B. Ratchford, Y.P. Zhao, Journal of Power Sources 204 (2012) 168–176.
[32] L.Q. Zhang, X.H. Liu, Y. Liu, S. Huang, T. Zhu, L.J. Gui, S.X. Mao, Z.Z. Ye, C.M. Wang, J.P. Sullivan, J.Y. Huang, ACS Nano 5 (2011) 4800–4809.
[33] J.Y. Huang, L. Zhong, C.M. Wang, J.P. Sullivan, W. Xu, L.Q. Zhang, S.X. Mao, N.S. Hudak, X.H. Liu, A. Subramanian, H.Y. Fan, L.A. Qi, A. Kushima, J. Li, Science 330 (2010) 1515–1520.
[34] F. Patolsky, G.F. Zheng, C.M. Lieber, Nature Protocols 1 (2006) 1711–1724.
[35] M.N. Obrovac, L. Christensen, Electrochemical and Solid-State Letters 7 (2004) A93–A96.
[36] Y.H. Yue, P. Liu, Z. Zhang, X.D. Han, E. Ma, Nano Letters 11 (2011) 3151–3155.
[37] C.K. Chan, R. Ruffo, S.S. Hong, R.A. Huggins, Y. Cui, Journal of Power Sources 189 (2009) 34–39.
[38] M.K.Y. Chan, B.R. Long, A.A. Gewirth, J.P. Greeley, The Journal of Physical Chemistry Letters 2 (2011) 3092–3095.

Matthew McDowell received his B.S. degree in materials science and engineering from the Georgia Institute of Technology in 2008, and he is now a graduate student in the Department of Materials Science and Engineering at Stanford University. His current research involves studying the physical, mechanical, and electrochemical properties of high-capacity battery electrode materials using a variety of techniques, including in-situ TEM.

Seok Woo Lee was born in Gongju, Republic of Korea in 1981. He received his B.S. degree in mechanical engineering from Pohang University of Science and Technology (POSTECH), Pohang, Republic of Korea, in 2003 and his Ph.D. degree in mechanical engineering from Korea Advanced Institute of Science and Technology (KAIST), Daejeon, Republic of Korea, in 2008. Currently, he is a postdoctoral researcher in the Department of Materials Science and Engineering at Stanford University. He has worked on microfluidics and micro actuators using MEMS fabrication, and is currently involved in studying the mechanical behavior of silicon anodes for lithium-ion batteries.

Chongmin Wang is a Senior Research Scientist at the Environmental Molecular Sciences Laboratory at Pacific Northwest National Laboratory. He possesses expertise in atomic level characterization/visualization of materials structure and physical/chemical behavior. He has consistently worked on correlating materials structural and functional properties with atomic and electronic structure and chemical composition; in particular, he has studied nanomaterials related to energy conversion, storage, and sustainability. Recently, he has focused on developing methods that enable in-situ atomic level observation of both chemical (catalytic processes), electrochemical processes (energy conversion and storage, such as lithium ion batteries), and mechanical behavior (such as stress-strain, impurity/dopant segregation, grain-boundary or interface mediated mass transport, defect clustering, and radiation damage) using aberration corrected HRTEM and HR-STEM. He has authored/co-authored 215 peer reviewed journal publications and has given more than 90 presentations.

Please cite this article as: M.T. McDowell, et al., The effect of metallic coatings and crystallinity on the volume expansion of silicon during electrochemical lithiation/delithiation, Nano Energy (2012), http://dx.doi.org/10.1016/j.nanoen.2012.03.004

Yi Cui received his B.S in chemistry at the University of Science and Technology of China in 1998 and his Ph.D. in chemistry at Harvard University in 2002. He went on to work as a Miller Postdoctoral Fellow at the University of California, Berkeley. In 2005, he became a professor in the Department of Materials Science and Engineering at Stanford University. He leads a group of researchers working on nanomaterials for energy, electronics and biotechnology. Among other honors, he has received the Wilson Prize from Harvard University (2011), the KAUST Investigator Award (2008), the ONR Young Investigator Award (2008), the MDV Innovators Award (2007) and the Technology Review World Top Young Innovator Award (2004).

Please cite this article as: M.T. McDowell, et al., The effect of metallic coatings and crystallinity on the volume expansion of silicon during electrochemical lithiation/delithiation, Nano Energy (2012), http://dx.doi.org/10.1016/j.nanoen.2012.03.004